6 April 2001

Chemical Physics Letters 337 (2001) 237–242

CHEMICAL PHYSICS LETTERS

www.elsevier.nl/locate/cplett

An intense pulsed electrical discharge source for OH molecular beams

M.C. van Beek *, J.J. ter Meulen

Department of Molecular and Laser Physics, University of Nijmegen, P.O. Box 9010, NL-6500 GL Nijmegen, Netherlands

Received 23 November 2000; in final form 5 February 2001

Abstract

In this Letter we describe and characterize a pulsed DC discharge source for a molecular beam of OH radicals. The absolute line-integrated OH density has been measured by cavity ring-down spectroscopy, while the off-axis distribution of the radicals has been determined by 1-dimensional laser-induced fluorescence spectroscopy. Combining both measurements the total OH centerline flux at the maximum of the pulse was determined to be $(2.2 \pm 0.1) \times 10^{17}$ molecules/sr s. No anomalous population distribution was found for the Λ-doublet components of the rotational ground state. © 2001 Elsevier Science B.V. All rights reserved.

1. Introduction

Because of their high reactivity, free radicals play a key role in the dynamics of many chemical reactions and numerous experiments have been reported on (half-)collisions involving these molecules. However, their high reactivity also causes difficulties in the generation of free radicals for laboratory studies. In particular, the radicals have to be produced in a low-pressure environment to prevent their immediate loss by unwanted reactions. The methods which have been used for the production of free radicals can be grouped into four categories: photolysis, pyrolysis, gas discharges and chemical reactions [1].

One of the most frequently studied radicals in molecular beam experiments is the OH molecule. The first intense continuous OH beam source reported was based on the chemical reaction $H + NO_2 \rightarrow OH + NO$ [2,3]. This source was estimated to yield a centerline flux of 2×10^{16} molecules/sr s [4]. Later, continuous OH molecular beams have been generated by radiofrequency [5] or corona [6,7] discharges of H_2O, while pulsed beams have been produced by photolysis of HNO_3 with 193 nm light [8,9]. Unfortunately no reliable estimates of the OH flux of these sources has been reported. In our laboratory an OH beam source has been developed based on a pulsed DC discharge in a H_2O/Ar jet at the beginning of the expansion into the vacuum chamber [10]. Compared to the other production methods, a pulsed discharge provides a simple, cheap, intense and stable OH source. To our knowledge the only other OH pulsed discharge sources have been reported by Bramble and Hamilton [11] and by Anderson et al. [12]. These sources have been used for spectroscopic studies of OH and OH–Ar in the free-jet expansion.

In this Letter we describe and characterize our OH source. There were several reasons for performing this experiment. First, the absolute flux of

* Corresponding author. Fax: +31-24-3653311.
E-mail address: mvbeek@sci.kun.nl (M.C. van Beek).

0009-2614/01/$ - see front matter © 2001 Elsevier Science B.V. All rights reserved.
PII: S0009-2614(01)00223-8

the molecular beams has to be known in order to determine absolute cross sections in crossed beam collision experiments. Secondly, from the obtainable flux the feasibility of specific OH beam experiments can be estimated. Thirdly, in previous experiments a remarkable difference in population between the OH Λ-doublet components of the lowest rotational states has been found when OH was produced in a pulsed discharge [10]. Since the energy spacing between these Λ-doublet states is only 0.05 cm^{-1} the population of these states is expected to be almost equal after the supersonic expansion. A large population difference in the beam can only be explained if there is a very strong propensity for one of the Λ-doublet states in the production of OH. Such a propensity has been observed for the photodissociation of H_2O by 157 nm light [13]. It should be noted that for the OH source described in this Letter a different pulsed valve has been used than in previous experiments [10]. The properties of the discharge, however, are similar.

2. Experimental

The discharge geometry is depicted schematically in Fig. 1. The OH beam is produced by expanding a 3% H_2O-in-Ar mixture at a total pressure of 800 mbar into a vacuum chamber. This mixture is obtained by flowing Ar through liquid water at room temperature (vapor pressure of 24 mbar) in a bubbler. For the expansion, a commercially available pulsed supersonic valve (R.M. Jordan) is used. The operation of this valve is based on the current-loop mechanism. It has a repetition rate of 10 Hz and a pulse duration of about 40 μs. On top of the standard nozzle with a diameter of 0.5 mm a stainless steel nozzle with an orifice of 0.2 mm and a conical shape is mounted. A 0.5 mm thick stainless steel ring with a diameter of 4 mm located on-axis 2.5 mm from the orifice is kept at a voltage of −2.4 kV. The OH radicals are produced by the dissociation of H_2O at the beginning of the expansion by the electrical discharge between the ring and the grounded valve body. This discharge is initiated by the rise of the local pressure when the valve opens; it automatically stops when the valve closes. The conical shape of the nozzle confines the discharge to the orifice. The current between the ring and the valve has a pulse length of 55 μs (FWHM) and a pulse maximum of 300 μA. During operation the average pressure in the vacuum chamber is 2×10^{-6} mbar. After production the OH radicals are cooled down to the lowest rotational state ($X^2\Pi_{3/2}$, $v = 0$, $J = 3/2$) during adiabatic expansion into the vacuum chamber. This state is split into two Λ-doublet components which are denoted by e (lower) and f (upper).

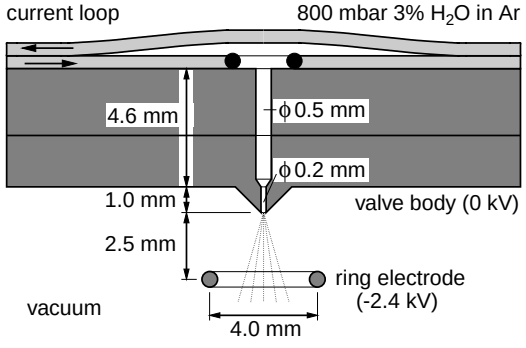

Fig. 1. Geometry of pulsed nozzle and discharge.

To investigate the characteristics of the OH beam, a laser beam crosses the molecular beam 2.3 cm downstream of the orifice. The relative spatial distribution as a function of the distance from the molecular beam axis was determined by saturated 1-dimensional laser-induced fluorescence (1D-LIF), and the absolute line-integrated OH density was measured by cavity ring-down spectroscopy (CRDS). For both experiments the $A^2\Sigma(v = 0) \leftarrow X^2\Pi(v = 0)$ transition around 308 nm was used. Since 94% of the OH radicals are in one of the Λ-doublet states of the rotational ground state, only these states are considered in this Letter [10]. The population of the e state is probed by the $P_1(1)$ transition, whereas the $Q_1(1) + Q_{21}(1)$ transitions were used to measure the population of the f state [14]. The laser light was produced by a dye-laser (Continuum TDL-60) operating with Sulforhodamine 640 dye and pumped by a 10 Hz Nd:YAG laser (Quantel 681C), and was frequency doubled in a KDP crystal. The resulting 308 nm light has an energy of 4 mJ/pulse, a bandwidth of 0.4 cm^{-1} and a pulse length of 5 ns. The diameter of the laser beam is about 5 mm.

2.1. 1-Dimensional LIF

The setup for the 1D-LIF measurements is depicted schematically in Fig. 2A. The fluorescence was measured spatially resolved by an intensified CCD camera (Princeton instruments ICCD-512-T) placed at a distance of 60 cm from the OH beam. With a Nikon UV 105 mm f/4.5 objective an area of 4×4 cm^2 could be imaged onto the 512×512 pixels of the CCD chip. Two Schott colored filters (UG11 and WG295) were mounted in front of the camera to suppress stray light from the laboratory and scattered light from the discharge. After the laser beam exits the vacuum chamber, the intensity is attenuated and the relative power is measured with a photomultiplier.

The images were measured with the laser frequency fixed at the center of the $P_1(1)$ or $Q_1(1)$ transition. A 3 mm diaphragm was used to cut off the low-energy wings of the laser beam. The power in the center of the laser beam was high enough to completely saturate these transitions. The fluorescence signal detected by the CCD chip was integrated over a period of 1.4 μs. Each final image consisted of 640 single shot images. The background (caused by the discharge, scattered laser light, stray light and dark current) was measured by tuning the laser out of resonance, and subtracted from the fluorescence images. The resulting fluorescence signal was integrated in the direction perpendicular to the laser beam to give the OH distribution along the laser beam.

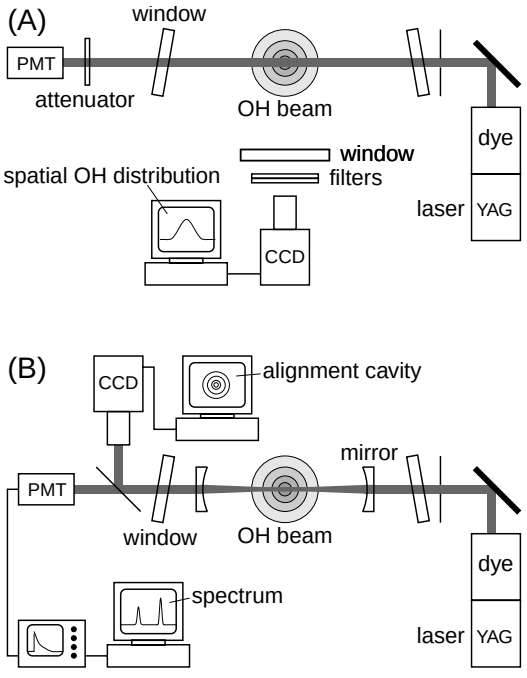

Fig. 2. Experimental setup for the saturated 1D-LIF measurements (A) and for the CRDS measurements (B). The direction of the OH beam, represented by the concentric circles, is perpendicular to the paper.

2.2. Cavity ring-down

The CRD setup is represented schematically in Fig. 2B. The cavity is formed by two highly reflective convex mirrors with a radius $R = 1$ m separated by 27 cm. The reflection coefficient of the mirrors was about 99.6%, which is rather low for CRDS experiments. We preferred to use older mirrors with a lower reflectivity since the ions produced in the discharge slightly damage the mirrors during the experiment. The ring-down time of the empty cavity was around 215 ns. The light leaking out of the cavity was detected by a fast photomultiplier tube (EMI 9235 Q) and visualized on a 10 bit 300 MHz oscilloscope (Yokogawa DL-42000). For each data point 8 pulses were averaged on the oscilloscope before a single exponential decay function was fitted to the ring-down signal. The decay time τ was stored on a PC as a function of the laser wavelength. In order to control the alignment of the cavity during the experiment a fraction of the light leaking out of the cavity was imaged onto an intensified CCD camera.

The laser frequency was scanned around the $P_1(1)$ and the $Q_1(1) + Q_{21}(1)$ transitions to determine the population of both the e and f Λ-doublet components of the rotational ground state at the maximum pulse intensity. The population of the excited rotational states was too low to obtain a reasonable signal-to-noise ratio. To prevent saturation effects the laser power was attenuated by a factor of 3 before entering the cavity. From the spatial distribution obtained in the 1D-LIF measurements the velocity distribution along the laser beam can be determined. This velocity distribution corresponds to a Doppler width of the absorption

lines of 0.048 cm^{-1}. This is much larger than the mode spacing of the cavity (0.0044 cm^{-1}) but smaller than the bandwidth of the laser ($\approx$0.4 cm^{-1}). Zalicki and Zare [15] have shown that if the laser bandwidth is larger than the absorption linewidth, the absolute number of molecules can be determined within an accuracy of 10% if the area of the absorption line is measured. For the analysis of the CRD spectra the laser bandwidth is approximated by a Gaussian frequency profile. The central position, width and area were fitted to the measured spectrum. Since the $Q_1(1)$ and $Q_{21}(1)$ lines partially overlap (the separation between these lines is 0.336 cm^{-1}), these lines cannot be analyzed independently. In the analysis we assume that the $Q_1(1)$ and $Q_{21}(1)$ lines have the same linewidth, and that the relative area is proportional to the relative absorption coefficient since both transitions probe the same ground state.

3. Results

In Fig. 3 the ratio of the fluorescence from the $P_1(1)$ to that of the $Q_1(1)$ transition is plotted as a function of the distance to the molecular beam axis. From the figure it can be seen that this ratio is nearly constant. The ratio slightly increases far away from the beam axis; however, this is also the region where the OH signals are very small and the ratio is very sensitive to variations in the background signal. Averaged over all distances the fluorescence ratio is equal to 0.665 ± 0.027, which is in perfect agreement with the ratio of 0.68 reported by Schreel et al. [10]. Since the spatial fluorescence distribution is similar for the detected states, the fluorescence from the different states is summed to provide the relative density distribution of the OH beam. Using the values for the total number of molecules along the detection path, determined with CRDS as is described in the following paragraphs, the relative density has been scaled to an absolute number density. This density distribution is also plotted in Fig. 3.

A typical CRDS spectrum is depicted in Fig. 4. From the integrated absorption of the $P_1(1)$ and the $Q_1(1) + Q_{21}(1)$ spectra the line-integrated number densities of the e and f states were determined. Both spectra were recorded 12 times. The standard deviation was about 5%; however, because the bandwidth of the laser is larger than the Doppler width a systematic error of the order of 10% can be made [15]. Therefore, the accuracy of the number densities is set to 10%. The line-integrated OH densities were found to be $N_{\text{line}}(\text{e}) = (3.32 \pm 0.34) \times 10^{11}$ and $N_{\text{line}}(\text{f}) = (3.68 \pm 0.37) \times 10^{11}$ molecules/cm^3 for the rotational ground state.

The ratio between the populations of the e and f states is 0.90 ± 0.14. This population ratio seems not to be in accordance with the fluorescence ratio of 0.665. However, in the interpretation of saturated LIF signals the degeneracy of the ground and excited states has to be taken into account by

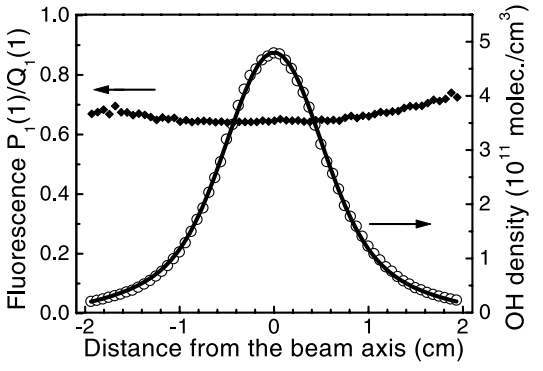

Fig. 3. Ratio of the fluorescence from the $P_1(1)$ and $Q_1(1)$ transition (◆), distribution of the OH radicals perpendicular to the molecular beam axis (○) and analytical fit to the distribution (gray line).

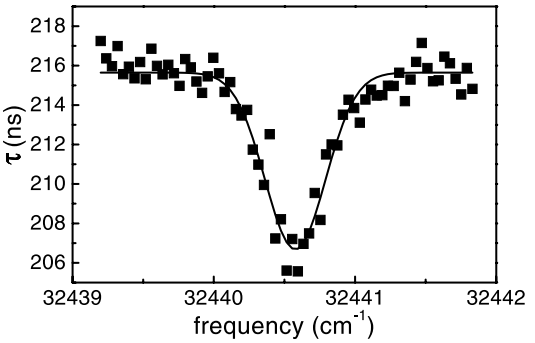

Fig. 4. Typical CRD spectrum of the $P_1(1)$ transition.

the so-called excitation rate factor. For unpolarized laser light this factor is given by [16,17]

$$\text{E.R.} = \frac{(2J'+1)}{(2J'+1)+(2J+1)}, \quad (1)$$

where J and J' are the angular momentum quantum numbers of the electronic ground and excited states, respectively. For the $Q_1(1)$ transition $J = 3/2$ and $J' = 3/2$, while for the $P_1(1)$ transition $J = 3/2$ and $J' = 1/2$. In order to calculate the relative population the fluorescence signals from the $Q_1(1)$ and $P_1(1)$ lines have to be divided by the corresponding excitation rate factors of $1/2$ and $1/3$, respectively. The resulting population ratio, as determined by saturated 1-dimensional LIF, is 1.00 ± 0.04. On the basis of both the CRD and the 1D-LIF results we conclude that the Λ-doublet states of OH are equally populated. Note that Anderson et al. [12] also found the population of these states to be equal in their pulsed discharge OH source. In the results obtained previously in our laboratory by Schreel et al. the excitation rate factors have been neglected in the interpretation of the saturated LIF results. If these factors are used in a reanalysis of these data a population ratio of 1.02 is found, which is consistent with the present investigation.

The total line-integrated OH density is given by a summation of the densities of the $\Omega = 3/2$, $J = 3/2$, e and $\Omega = 3/2$, $J = 3/2$, f state divided by 0.94 since approximately 6% of the OH molecules are distributed over other rotational states. For our OH source we find: $N_{\text{line}}(\text{OH}) = (7.4 \pm 0.6) \times 10^{11}$ molecules/cm^2. This value has been used to scale the relative OH distribution measured by 1D-LIF to absolute number densities. The total centerline OH density 2.3 cm downstream of the nozzle is $(5.1 \pm 0.4) \times 10^{11}$ molecules/cm^3. The OH beam velocity has been determined to be 885 ± 80 m/s [18]. With this velocity the centerline flux was calculated to be $I = (2.2 \pm 0.1) \times 10^{17}$ molecules/sr s. Assuming a $1/z^2$ dependency, where z is the distance from the nozzle, the density 1 cm downstream of the nozzle can be calculated to be $(2.7 \pm 0.2) \times 10^{12}$ molecules/cm^3. This value is of the same order of magnitude as the value of 3.9×10^{12} molecules/cm^3 which was reached in a pulsed slit nozzle discharge source described by Anderson et al. [12].

From the off-axis OH distribution depicted in Fig. 3 the angular distribution of the OH beam was calculated, and scaled to the measured OH centerline flux. The resulting angle-dependent flux can be described by a superposition of two Gaussian functions,

$$I(\theta) = 1.65\exp[-11.6\theta^2] + 0.55\exp[-03.6\theta^2], \quad (2)$$

where $I(\theta)$ is the OH flux in 10^{17} molecules/sr s and θ is the angle between the average OH beam direction and the direction in which the flux is calculated.

The OH density has also been measured as a function of time by 1D-LIF. The results are depicted in Fig. 5. Except for a small tail, the pulse shape can be described by a Gaussian distribution with a width of 50 μs. This value is somewhat longer than the opening time of the valve (about 40 μs) due to the velocity spread in the beam.

The OH production efficiency can be defined as the ratio between the OH flux and the H_2O flux when the discharge is off. This H_2O flux was estimated using the expression for an ideal continuous free jet given by Miller [19]. Since the density is proportional to $1/z^2$, in the expansion as well as in the beam, this expression equally holds for an ideal

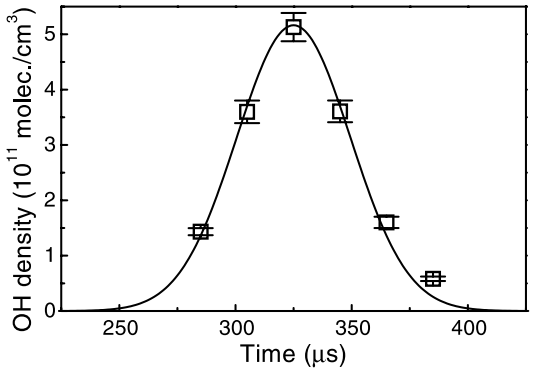

Fig. 5. OH centerline density as a function of time. The measured values are represented by a □, the solid line represents a fitted Gaussian distribution. At 2.3 cm from the orifice the pulse has a width (FWHM) of 50 μs. The measured time is the time between the triggering of the pulsed valve and the firing of the laser. This time includes the delay of 250–300 μs between the trigger signal and the opening of the valve.

molecular beam. For H_2O seeded in Ar we find a centerline flux of $I(H_2O) = 2.0 \times 10^{18}$ molecules/sr s at the present source conditions. This gives an OH production efficiency of 11%. Note that this is a lower limit for the production efficiency. First, since the pulsed nozzle has a rather long and narrow exit the H_2O density at the orifice will be lower than that for an ideal nozzle. Secondly, although the temperature of the nozzle is not known, it will be higher than room temperature, which leads to a lower H_2O density at the same pressure. Moreover, we use a pulsed source, whereas the expression is valid for a continuous source, and we have neglected any influence of the discharge ring, the discharge itself and the background gas. Hence the actual OH production efficiency is expected to be significantly higher than 11%.

4. Conclusions

We have investigated the production of OH in a pulsed DC discharge. This discharge provides an easy, cheap, intense and stable source of rotationally cold $OH(X^2\Pi)$ radicals. At the maximum of the pulse, the total OH centerline flux has been determined to be $I = (2.2 \pm 0.1) \times 10^{17}$ molecules/sr s, an order of magnitude larger than the flux for a continuous beam source based on the chemical reaction between H and NO_2 [4]. The angular dependence of the OH beam flux in the present setup is given by $I(\theta) = (1.65\exp[-11.6\theta^2] + 0.55\exp[-3.6\theta^2]) \times 10^{17}$ molecules/sr s. The OH production efficiency in our pulsed discharge is at least 11%. The total population and the angular distribution of both Λ-doublet states of the rotational ground state were found to be equal. This indicates that if a Λ-doublet propensity exists in the production of OH this is thermalized in the expansion.

Acknowledgements

The authors thank Rogier Evertsen for his help during the experiment and the interpretation and Dr. Nico Dam for stimulating discussions.

References

[1] J.C. Whitehead, Rep. Prog. Phys. 59 (1996) 993.
[2] J.J. ter Meulen, A. Dymanus, Astrophys. J. 172 (1972) L21.
[3] J.J. ter Meulen, W.L. Meerts, G.W.M. van Mierlo, A. Dymanus, Phys. Rev. Lett. 36 (1976) 1031.
[4] J.J. ter Meulen, Ph.D. Thesis, University of Nijmegen, The Netherlands, 1976.
[5] M. Alagia, N. Balucani, P. Casavecchia, D. Stranges, G.G. Volpi, J. Chem. Phys. 98 (1993) 2459.
[6] A.T. Droege, P.C. Engelking, Chem. Phys. Lett. 96 (1983) 316.
[7] T.D. Hain, M.A. Weibel, K.M. Backstrand, T.J. Curtiss, J. Phys. Chem. A 101 (1997) 7674.
[8] P. Andresen, N. Aristov, D. Beushausen, H.W. Lülf, J. Chem. Phys. 95 (1991) 5763.
[9] D.M. Sonnenfroh, R.G. Macdonald, K. Liu, J. Chem. Phys. 93 (1991) 1478.
[10] K. Schreel, J. Schleipen, A. Eppink, J.J. ter Meulen, J. Chem. Phys. 99 (1993) 8713.
[11] S.K. Bramble, P.A. Hamilton, Chem. Phys. Lett. 170 (1990) 107.
[12] D.T. Anderson, S. Davis, T.S. Zwier, D.J. Nesbitt, Chem. Phys. Lett. 258 (1996) 207.
[13] P. Andresen, G.S. Ondrey, B. Titze, E.W. Rothe, J. Chem. Phys. 80 (1984) 2548.
[14] G.H. Dieke, H.M. Crosswhite, J. Quant. Spectrosc. Radiat. Transfer 2 (1962) 97.
[15] P. Zalicki, R.N. Zare, J. Chem. Phys. 102 (1995) 2708.
[16] D.R. Guyer, L. Hüwel, S.R. Leone, J. Chem. Phys. 79 (1983) 1259.
[17] J.M. Hossenlopp, D.T. Anderson, M.W. Todd, M.I. Lester, J. Chem. Phys. 109 (1998) 10707.
[18] M.C. van Beek, J.J. ter Meulen, M.H. Alexander, J. Chem. Phys. 113 (2000) 628.
[19] D.R. Miller, in: G. Scoles (Ed.), Atomic and Molecular Beam Methods, Oxford University Press, New York, 1988.